

See discussions, stats, and author profiles for this publication at: <https://www.researchgate.net/publication/229811688>

Synthesis, Characterization and Molecular Conformation of Syndiotactic 1,2 Polypentadiene: The Cis Polymer

ARTICLE in *MACROMOLECULES* · OCTOBER 2005

Impact Factor: 5.8 · DOI: 10.1021/ma047604y

CITATIONS

8

READS

3

9 AUTHORS, INCLUDING:



Giovanni Ricci

Italian National Research Council

94 PUBLICATIONS 1,160 CITATIONS

SEE PROFILE



Raniero Mendichi

Italian National Research Council

119 PUBLICATIONS 2,339 CITATIONS

SEE PROFILE



Paolo Arosio

University of Milan

41 PUBLICATIONS 614 CITATIONS

SEE PROFILE



Stefano Valdo Meille

Politecnico di Milano

192 PUBLICATIONS 4,053 CITATIONS

SEE PROFILE

Synthesis, Characterization and Molecular Conformation of Syndiotactic 1,2 Polypentadiene: The Cis Polymer

Giovanni Ricci,* Enrica Alberti, Lucia Zetta,* Tiziano Motta, Fabio Bertini, Raniero Mendichi, Paolo Arosio,[†] Antonino Famulari,[†] and Stefano Valdo Meille*,[†]

CNR–Istituto per lo Studio delle Macromolecole (ISMAC), via E. Bassini 15, I-20133 Milano, Italy, and Dipartimento di Chimica, Materiali ed Ingegneria Chimica del Politecnico di Milano, via L. Mancinelli 7, I-20131 Milano, Italy

Received November 19, 2004; Revised Manuscript Received June 20, 2005

ABSTRACT: (*Z*)-1,3-pentadiene has been polymerized with the CpTiCl₃–MAO system at –78 °C to a polymer consisting exclusively of *cis*-1,2 units and having a syndiotactic structure. The polymer has been characterized by NMR (¹³C and ¹H in solution and ¹³C in the solid state), IR, DSC, GPC, X-ray, and molecular modeling techniques, comparing its conformational and structural properties with those of other 1,2-syndiotactic polymers. Diffraction and NMR data are consistent with the idea that a single crystalline polymorph prevails in the studied samples. The solid-state NMR results allow us to exclude the all-trans (*T*₄) conformation for *cis*-1,2 syndiotactic polypentadiene and indicate a nonuniform helix of the *T*₂G₂ type as most plausible, although other possibilities such as the (*T*₆G₂*T*₂G₂)_{*n*} conformation cannot be completely ruled out. These conclusions follow from the fact that two conformationally distinct methylene C1 carbons are observed, which experience, respectively, zero and two γ-gauche interactions. Isolated chain molecular mechanics calculations too show that both (*T*₂G₂)₂ and (*T*₆G₂*T*₂G₂)_{*n*} conformations are of comparable stability, while the more extended all-trans (*T*₄) arrangement has significantly higher internal energy, at variance with the situation found in most 1,2-syndiotactic polydienes. Simple qualitative considerations on the steric conflicts involving terminal *cis* methyls of the side chains of adjacent monomer units in the all-trans conformation rationalize this result.

Introduction

Since 1955, when Natta et al.¹ first synthesized a polymer from 1,3-pentadiene, the *trans*-1,4 isotactic isomer, several new polypentadienes have been prepared using catalyst systems based on transition metals. However, of the series of 10 stereoregular polypentadienes that can be predicted (Figure 1), only four were initially obtained: isotactic and syndiotactic *cis*-1,4,² isotactic *trans*-1,4,³ and syndiotactic *trans*-1,2.⁴ The 1,4 polymers were found to be crystalline by X-ray analysis, while the 1,2 polymer was found to be amorphous. Preliminary characterization of these polymers in terms of microstructure has been accomplished by Beebe et al.⁵ through a combination of IR spectroscopy, X-ray diffraction, and NMR spectroscopy.

In the 1980s, homogeneous catalysts based on transition metallocene compounds and methylaluminoxane have been developed that are capable of producing poly-α-olefins with a high degree of stereoregularity and narrow molecular weight distribution.⁶ Our first attempt to use the CpTiCl₃–MAO catalyst system to polymerize 1,3-dienes gave quite interesting results, yielding highly stereoregular polymers from various types of monomers, such as 2,3-dimethyl-1,3-butadiene, (*E*)-2-methyl-1,3-pentadiene, and 4-methyl-1,3-pentadiene.⁷ In particular, from (*Z*)-1,3-pentadiene, a monomer which was never polymerized before, polymers with different structure were obtained, depending on the polymerization temperature. A *cis*-1,4 polymer was obtained at room temperature, a mixed *cis*-1,4/*cis*-1,2

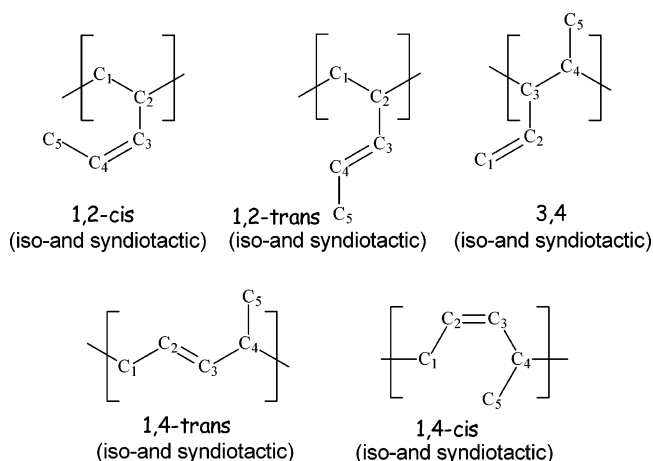


Figure 1. Possible stereoregular polymers obtainable from 1,3-pentadiene.

polymer at 0 °C, and a *cis*-1,2 syndiotactic polymer at –30 °C. Hence, for the first time, *cis*-1,2 syndiotactic polypentadiene was prepared.⁸ The results obtained in the polymerization of 1,3-dienes with CpTiCl₃–MAO were extremely useful also from a mechanistic point of view because they allowed us to address the issue of the influence of monomer structure on polymerization chemoselectivity.⁹

The polymerization of (*Z*)-1,3-pentadiene was carried out at –78 °C in the present investigation because in general, in the polymerization of 1,3-dienes with transition metal catalysts, a low polymerization temperature has the effect of improving the stereoregularity, the crystallinity, and the molecular weight of the polymers obtained. Unfortunately, even under these conditions, only a relatively low-molecular-weight 1,2-polypentadiene was obtained, which has been extensively char-

* Authors to whom correspondence should be addressed. E-mail: giovanni.ricci@ismac.cnr.it (G.R.); lucia.zetta@ismac.cnr.it (L.Z.); valdo.meille@polimi.it (S.V.M.).

[†] Dipartimento di Chimica, Materiali ed Ingegneria Chimica del Politecnico di Milano.

acterized by nuclear magnetic resonance (NMR) in solution and in the solid state, infrared spectroscopy (IR), differential scanning calorimetry (DSC), gel permeation chromatography (GPC), molecular mechanics, and as far as possible, by X-ray diffraction techniques. On the basis of these data, a *cis*-1,2 syndiotactic structure was confirmed for the newly synthesized polypentadiene. Because of the low molecular weight of the synthesized polymer, we were, however, unable to obtain significant orientation in fibers or films. Without fiber repeat information, it proved impossible so far to propose, on the basis of the diffraction data, reliable conformational models. Substantial information concerning the conformation of the new 1,2-polypentadiene in the crystalline state was, however, provided by solid-state high-resolution ^{13}C NMR spectroscopy on the basis of considerations of the γ -gauche shielding interactions that indeed markedly depend on polymer conformation. These data, along with resonance multiplicities and molecular modeling results, allow the ruling out of the all-*trans* T_4 main-chain conformation, suggesting rather a distorted T_2G_2 helical conformation or, with lower probability, a $\text{T}_6\text{G}_2\text{T}_2\text{G}_2$ structure like the one determined for the closely related 1,2-syndiotactic poly(4-methyl-1,3-pentadiene). Our modeling results represent a substantial, consistent complement to those reported by Pirozzi et al.¹⁰ for the same polymers by molecular mechanics calculations. The influence of the *cis* or *trans* side-chain double-bond configuration on the polymer main-chain conformation has been finally examined, with reference to calculations and experimental data pertaining to the crystalline *trans*-1,2 syndiotactic polypentadienes¹¹ recently prepared in our laboratory.

Experimental Section

Materials. CpTiCl_3 (Strem Chemicals, 99% pure) and methylaluminoxane (MAO) (Crompton, 10 wt % solution in toluene) were used as received. Toluene (Baker, >99% pure) was refluxed over Na for ca. 8 h, then distilled and stored over molecular sieves under dry nitrogen; pentane (Carlo Erba, >99%) was refluxed over K for ca. 8 h, then distilled and stored over molecular sieves under dry nitrogen. (*Z*)-1,3-pentadiene (Fluka, >98% pure) was refluxed over CaH_2 for ca. 2 h, then distilled trap-to-trap and stored under dry nitrogen.

Polymerization. Toluene (3.75 mL) and (*Z*)-1,3-pentadiene (5 mL, 3.46 g) were introduced in a 50-mL dried flask. The solution was cooled to -78°C in a dry ice/acetone bath, then MAO (2.5×10^{-2} mol, 15.75 mL) and CpTiCl_3 (5×10^{-5} mol, 5.5 mL of a 2-mg/mL toluene solution) were added in the order given. The polymerization was terminated with methanol after about four weeks, the polymer was coagulated and repeatedly washed with a large excess of methanol, and then dried in a vacuum at room temperature (yield 2.7 g, 78% conversion).

Polymer Fractionation. The crude polymer (2 g) was fractionated by extraction with two different boiling solvents (acetone for 24 h and pentane for 24 h). The following polymeric fractions were isolated: acetone soluble fraction, 0.22 g (11% of the initial polymer); pentane soluble fraction, 1.30 g (65%); insoluble residue, 0.48 g (24%).

Polymer Characterization. The crude polymer and the isolated polymer fractions were characterized by IR, NMR, DSC, GPC, and X-ray techniques.

IR spectra were carried out on a Bruker IFS 48 instrument using films on KBr disks; polymer films were obtained by deposition from benzene solutions.

^{13}C and ^1H NMR spectra were performed with Bruker AM 270 and Avance 500 spectrometers. The spectra were obtained in CDCl_3 at 22°C , and chemical shifts were referenced to TMS as an internal standard. The concentration of the polymer solutions ranged from 3 to 10 wt %.

The heteronuclear shift-correlated two-dimensional (2D) NMR spectrum¹² was obtained with quadrature detection in both dimensions, using polarization transfer from ^1H to ^{13}C via $J_{\text{H,C}}$, with proton decoupling. In the ^{13}C domain, 11 000 Hz were sampled over 2048 data points, then zero filled to 4096. In the ^1H domain, 1200 Hz over 256 traces were accumulated (1024 scans for trace), then zero filled to 512 before Fourier transformation; the relaxation delay was 2 s. The delay for polarization transfer was 3.8 ms, corresponding to a $J_{\text{H,C}}$ value of 130 Hz.

The 2D double-quantum-filtered correlated spectroscopy DQF COSY spectrum¹³ was acquired with a sweep width of 2400 Hz over 2048 data points in the F_2 domain, and 1000 Hz over 1024 traces in the F_1 domain. The 2D spectra were resolution-enhanced with a $\pi/3$ -shifted squared sine-bell in both dimensions.

Solid-state NMR ^{13}C spectra were recorded using a Bruker AVANCE spectrometer operating at 400 MHz for proton and a 4-mm double-bearing MAS probe. The spectra were recorded at room temperature, with 90° pulse lengths of about 4 μs and were transformed using a line broadening of 10 Hz. The number of scans (NS) are indicated in figure captions. The ^{13}C single pulse excitation (SPE) spectrum was recorded using a recycle time of 10 s in order to select the signals arising from the most mobile moieties. For the ^{13}C cross-polarization and magic-angle spinning (CPMAS) NMR experiments, recycle times of 5 s, contact times of 1 ms, and a spinning rate of 5 kHz were used.

DSC scans were performed on a Perkin-Elmer Pyris 1 instrument. The samples, typically 3–5 mg, were placed in a sealed aluminum pan, and the measurements were carried out in a nitrogen atmosphere using a heating rate of $20^\circ\text{C}/\text{min}$.

The molecular weight averages and the molecular weight distribution (MWD) were obtained by a GPCV 2000 system (from Waters) using two on-line detectors: a differential viscometer and a refractometer. The experimental conditions consisted of two PLgel Mixed C columns, chloroform as the mobile phase, 0.6 mL/min of flow rate, and 35°C temperature. The calibration of the GPC system was constructed by 18 narrow MWD polystyrene standards with the molar mass ranging from 162 to $3.3 \cdot 10^6$ g/mol.

X-ray diffraction patterns were recorded using graphite-monochromated $\text{Cu K}\alpha$ radiation ($\lambda = 1.54179 \text{ \AA}$) on a Bruker P4 diffractometer equipped with a HiStar 2D detector. The sample-to-detector distance was about 10 cm. Some measurements were performed on a Bruker Nanostar system, equipped with mirror focusing, a HiStar 2D detector, and a WAXS attachment with a sample-to-detector distance of about 3 cm. Unoriented patterns were obtained using polymer powders pressed into a glassy capillary. Attempts to draw oriented fibers of the polymer failed, possibly because of the relatively low molecular weight.

Conformational Analysis. Molecular mechanics calculations have been performed to investigate the plausible stationary points of the potential energy surface without imposing constraints on the isolated main-chain conformation. The Chem3D suite of programs has been employed, adopting the MM2 force field¹⁴ in order to minimize the effects of spurious intrachain nonbonding interactions. The calculations have been carried out using 12 and 24 monomeric units chain fragments for the T_4 , the T_2G_2 , and the $\text{T}_6\text{G}_2\text{T}_2\text{G}_2$ main-chain models. Starting backbone geometries with standard torsion angles, i.e., 60° and 180° , and the side chains initially in an idealized skew conformation, have been assumed. The number of monomeric units in the calculations ensured minor terminal group effects, which were appropriately estimated and eliminated in the evaluation of internal energies. The unconstrained MM2 results have been complemented by further molecular mechanics calculations involving periodical conditions, with and without symmetry constraints, allowing modeling of infinite isolated polymer molecules. In this second step, the geometries found in the central chemical repeat units of the unconstrained MM2 minimizations were used as starting points for the energy minimization, and the PCFF force field

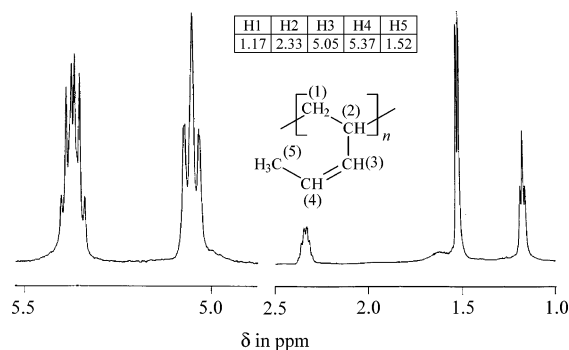


Figure 2. ^1H NMR (500 MHz) spectrum of *cis*-1,2 syndiotactic polypentadiene obtained at -78°C with the system CpTiCl_3 –MAO.

as implemented in the Materials Studio package¹⁵ has been adopted.

To evaluate the feasibility of significant deviations of the side-chain torsion angle (see Figure 14) from the skew conformation minimum, suggested by NMR, structural data, and molecular mechanics results, *ab initio* calculations were performed to determine the rotational barrier energies around the skew conformation. The energy of the system was optimized by fixing the ϕ angle in a range of $\pm 100^\circ$ around the global minimum (corresponding to skew conformation) in steps of 10° and relaxing all the other geometrical parameters. The GAUSSIAN suite of programs¹⁶ was employed by adopting RHF/6-31G**, MP2/6-31G**, and DFT/6-31G** levels of the theory.

Results and Discussion

Figure 2 reports the ^1H NMR spectrum of the polypentadiene obtained with the CpTiCl_3 –MAO system at -78°C . The signals were assigned on the basis of chemical shift values (aliphatic and olefinic protons) and multiplicity. H1 at 1.17 ppm is a triplet due to an equal vicinal coupling constant with the two covalently bonded methylenes; H2 at 2.33 ppm is a multiplet due to vicinal coupling constants with the H1 and H3; H3 at 5.05 is a triplet due to the two adjacent methylenes H2 and H4; H4 at 5.37 ppm is a doublet of quartets due to the vicinal couplings with H3 and H5, respectively; H5 is a doublet at 1.52 ppm due to the vicinal coupling constant with H4. This assignment is further confirmed by the COSY spectrum, as indicated in Figure 3. Specifically, the correlation between the methyl protons (H5) and the olefinic methyne proton (H4) is indicative of a 1,2 structure of the polymer because, in both the 1,4 and the 3,4 structures, the methyl group is bound to an aliphatic methyne group (see Figure 1). In the ^1H NMR spectrum (Figure 2), the coupling constant of the two olefinic protons (H3 and H4) is ca. 11 Hz, and this is consistent with a *cis* structure of the double bond. This evidence is confirmed by the IR spectrum (Figure 4), which shows the typical band at 725 cm^{-1} due to the *cis*-1,2 structure.^{2b,5} Moreover, in the ^1H NMR spectrum (Figure 2), the resonance of the methylene protons (H1) is a false triplet, indicating that the two protons are isochronous and that the polymer has a syndiotactic structure.¹⁷

Figure 5 shows the ^{13}C NMR spectrum of the polymer consisting of five sharp resonances, which were assigned as indicated on the basis of homonuclear (DEPT ^{13}C NMR spectrum, not shown) and heteronuclear experiments. In particular, the ^{13}C – ^1H heteronuclear correlated 2D experiment (Figure 6) enabled us to distinguish the two olefinic carbons, C3 and C4, on the basis of the unambiguous proton assignment.

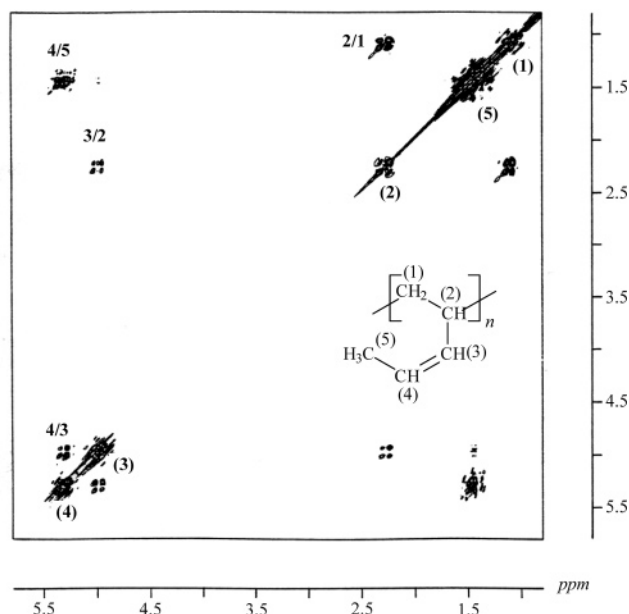


Figure 3. Two-dimensional DQF COSY (270 MHz) spectrum of *cis*-1,2 syndiotactic polypentadiene obtained with CpTiCl_3 –MAO system at -78°C .

The molecular weight of the crude polymer is $15\,730\text{ g mol}^{-1}$ (Figure 7). The MWD of the polymer is relatively narrow: the polydispersity index D ($D = M_w/M_n$ where M_n and M_w denotes respectively the numeric and the weight average of the molecular weight) is about 1.7, indicating that the polymerization occurs with a single-site catalyst.

The DSC thermogram of the crude sample (Figure 8a) shows a broad endothermic transition that spans the temperature range from 60 to 135°C (with a heat flow of 27 J/g); two endothermic peaks are observed, respectively centered at 83°C and 105°C , indicating the substantial crystallinity of the polymer but also pointing to the possible existence of different crystalline modifications.

This behavior can be better understood with reference to the X-ray diffraction data; comparison between patterns recorded at room temperature and at 130°C , i.e., above the melting temperature, allow estimation of the polymer degree of crystallinity at about 0.5 (Figure 9a). Attempts to obtain oriented fibers or films, to determine the fiber repeat and investigate the crystal structure by X-ray diffraction, were unsuccessful, most probably because of the relatively low molecular weight of the polymer.

With the aim of obtaining polymeric fractions characterized by a higher molecular weight, the crude polymer was fractionated as described in the Experimental Section. The different isolated fractions (acetone soluble, pentane soluble, and residue) were found to have the same microstructure, as indicated by their ^{13}C NMR (not shown). X-ray diffraction spectra (Figure 9b) suggest that the crystallinity of the as-precipitated fractions varies to some extent, while distinct thermal behaviors (Figure 8) and molecular weights (Figure 7) are apparent.

The acetone-soluble fraction exhibits a broad low-temperature melting endotherm centered at 83°C with a heat flow of 14 J/g . The pentane-soluble fraction presents an endothermic peak at 108°C ($\Delta H = 28\text{ J/g}$). Finally, the melting of the residue occurs at 125°C with a heat flow of 30 J/g . Thus, for the three fractions, the

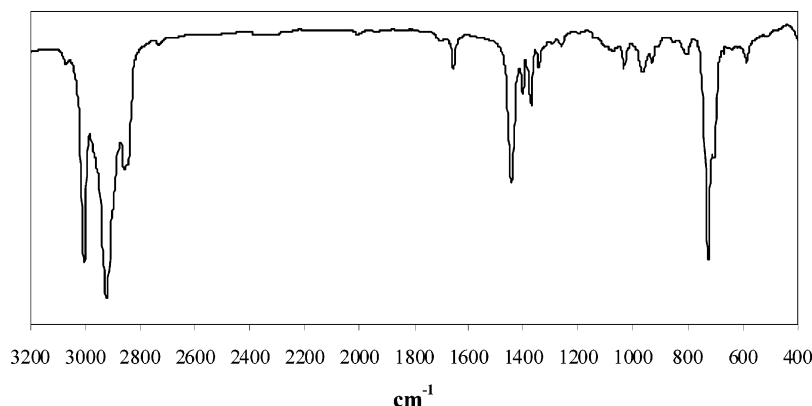


Figure 4. IR spectrum of *cis*-1,2 syndiotactic polypentadiene obtained with CpTiCl_3 -MAO system at -78°C .

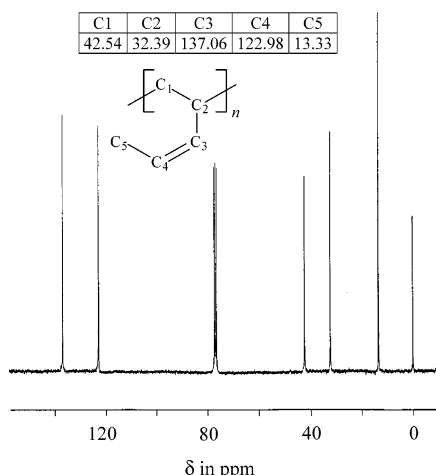


Figure 5. ^{13}C NMR (67 MHz) spectrum of *cis*-1,2 syndiotactic polypentadiene obtained with CpTiCl_3 -MAO system at -78°C .

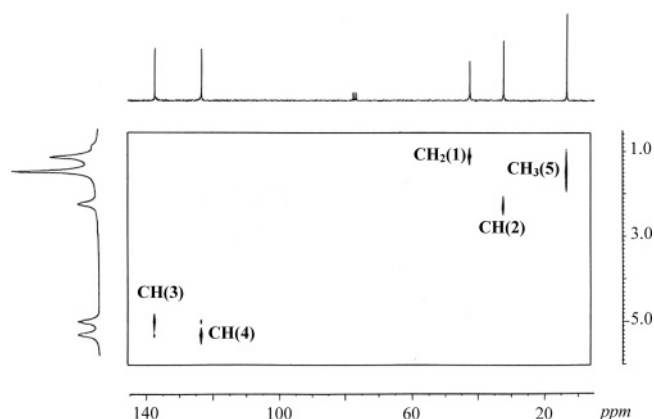


Figure 6. Two-dimensional $^{13}\text{C}/^1\text{H}$ (67 MHz) heteronuclear correlated spectrum of *cis*-1,2 syndiotactic polypentadiene obtained with CpTiCl_3 -MAO system at -78°C .

melting temperatures and enthalpies of fusion increase upon increasing the molecular weight (Figure 8). The acetone-soluble, the pentane-soluble, and the residue fractions have a M_w average value of 4860, 15 960, and 25 270 g/mol, respectively (Table 1). As already mentioned, the DSC results could possibly suggest the occurrence of different crystalline phases in the unfractionated polymer and in the three fractions. On the contrary, the X-ray diffraction profiles of the different fractions are very similar, implying that, with high probability, a single crystalline phase is present or is largely dominant in all the samples because the co-

presence of different polymorphs in exactly the same proportions is unlikely.

Because fibers suitable for X-ray diffraction studies could not be obtained even with the higher-molecular-weight fractions, we had to resort to ^{13}C NMR spectroscopy and molecular modeling to attempt to clarify the crystalline conformation of *cis*-1,2 syndiotactic polypentadiene. Figure 10a shows the ^{13}C SPE spectrum of the crude polymer, whereas Table 2 shows the peak assignments obtained by comparison with the solution ^{13}C NMR spectrum. In the ^{13}C SPE spectrum, broad signals around 40 and 48 ppm indicate the presence of some polymer in the amorphous phase. The peak at about 13 ppm (C5) is particularly intense and indicates the existence of a population of methyl side groups undergoing rapid rotation along the C–C bond axis. Figure 10b shows the ^{13}C CPMAS spectrum of the crude polymer. This experiment selects the most hindered carbons that correspond to the crystalline fraction of the polymer. The most evident difference with respect to the NMR solution spectrum is the splitting of all the peaks. In principle, this multiple splitting of single carbons may arise from different chemical environments coexisting in a single crystalline phase, or from co-presence of different crystalline forms in the sample. To distinguish between these two hypotheses, the ^{13}C CPMAS spectra of the three polymer fractions with different molecular weight and melting point were recorded and are shown in Figure 11. The features are identical to those observed for the whole polymer, thus confirming the first hypothesis, which is also consistent with the diffraction results (vide supra) and suggesting that the carbons in the polymer experience more than one local chemical environment.

Two resonances are observed for the C1 methylene carbon at 39.48 and 47.37 ppm: the separation of about 8 ppm in chemical shift suggests that two conformational environments differing for two γ -gauche effects occur.¹⁸ This signal splitting is in agreement with a $(\text{T}_2\text{G}_2)_2$ conformation (see Figure 12a), while it clearly rules out the all-trans T_4 conformation, in which only one signal is expected because of the conformational equivalence of all the C1 carbons (see Figure 13a). The same signal splitting has already been encountered in syndiotactic polymers adopting helix conformation of the T_2G_2 kind, in which the methylene carbons are conformationally distinct. In fact, the methylene carbons at the center of the *tggt* sequence are trans to both the methine carbons in γ -position, while in the *gttg* sequence, they are in a gauche arrangement, with both the methine carbons in γ -position (see Figure 12a).

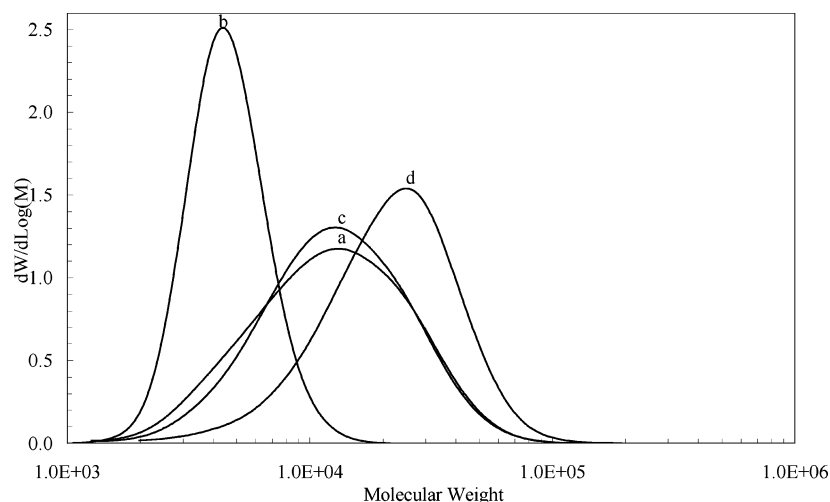


Figure 7. Comparison of the MWD, from GPC, of the different *cis*-1,2 syndiotactic polypentadiene fractions: (a) crude polymer, (b) acetone soluble fraction, (c) pentane soluble fraction, and (d) residual fraction.

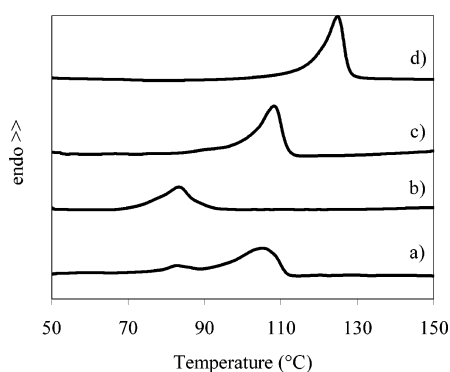


Figure 8. DSC thermograms of *cis*-1,2 syndiotactic polypentadiene obtained with CpTiCl_3 –MAO system at $-78\text{ }^\circ\text{C}$: (a) crude polymer, (b) acetone soluble fraction, (c) pentane soluble fraction, and (d) residual fraction.

However, a rigorously $(\text{T}_2\text{G}_2)_2$ conformation is not supported by the multiplicity observed for the C2 methine, whose 1.9-ppm splitting indicates the occurrence of at least two distinct C2 carbons in nonequivalent monomeric units. We emphasize that, in a regular T_2G_2 structure (Figure 12a), this carbon is expected to give a single signal because, lying at the center of symmetry-related *ttgg* sequences, it always experiences a trans and a gauche backbone conformation.

Moreover, the presence of three well-resolved peaks for the olefinic carbon C3 and C4 (1.6–2 ppm splitting) suggests the existence of at least three types of carbon environments, and again, it is in contrast with a uniform $(\text{T}_2\text{G}_2)_2$ structure for which only one signal would be expected for each olefin carbon.

A possible reason for the splitting might arise from conformational distortions. In the presence of a non-uniform helix with backbone torsion angles differing from the regular ones, the methine carbons could be nonequivalent because of different γ -gauche interactions deriving from distinct values of the gauche torsion angles. An analogous splitting of about 1.5 ppm was also observed by De Rosa et al.¹⁹ in the crystalline form of syndiotactic poly(4-methyl-1-pentene); in that case, the helical conformation was described with a complex nonuniform helix. The crystal structure of isotactic poly(1-butene) form I²⁰ and the three crystalline forms of isotactic poly(4-methyl-1-pentene)²¹ provide further examples in which the C2 methine signal is split because

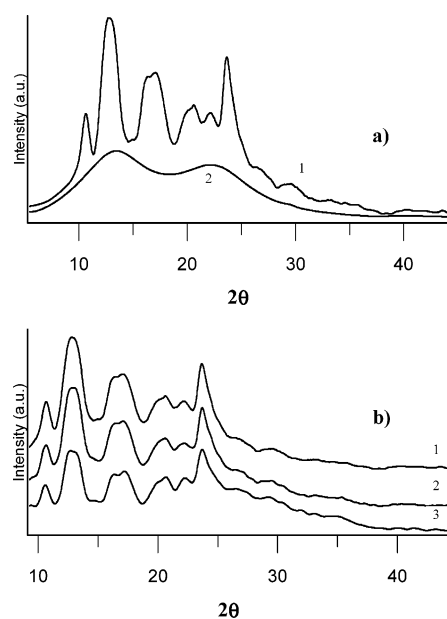


Figure 9. X-ray powder spectra of *cis*-1,2 syndiotactic polypentadiene obtained with CpTiCl_3 –MAO system at $-78\text{ }^\circ\text{C}$: (a) crude polymer at room temperature (1) and at $130\text{ }^\circ\text{C}$ (2); and (b) crude polymer (1), acetone soluble fraction (2), and residual fraction (3).

Table 1. Summary of the GPC Characterization

sample	M_w g/mol	D
crude polymer	15730	1.7
acetone soluble	4860	1.2
pentane soluble	15960	1.6
residue	25270	1.5

of the strong dependence of the γ -gauche shielding effect on the torsion angle value. In principle, the same conformational distortions of the main chain should affect the C1 resonances, possibly causing further signal splitting, but this was not observed.

On the other hand, the multiplicity observed for C2, C3, and C4 (but not C1) would be in favor of the $\text{T}_6\text{G}_2\text{T}_2\text{G}_2$ conformation (see Figure 12b) already observed for the metastable form IV²² of polypropylene and for the stable polymorph of the 1,2-syndiotactic poly(4-methyl-1,3-pentadiene),²³ a polymer which is very closely related to the system we are investigating. Indeed, all these carbons occur for the $\text{T}_6\text{G}_2\text{T}_2\text{G}_2$ conformation in

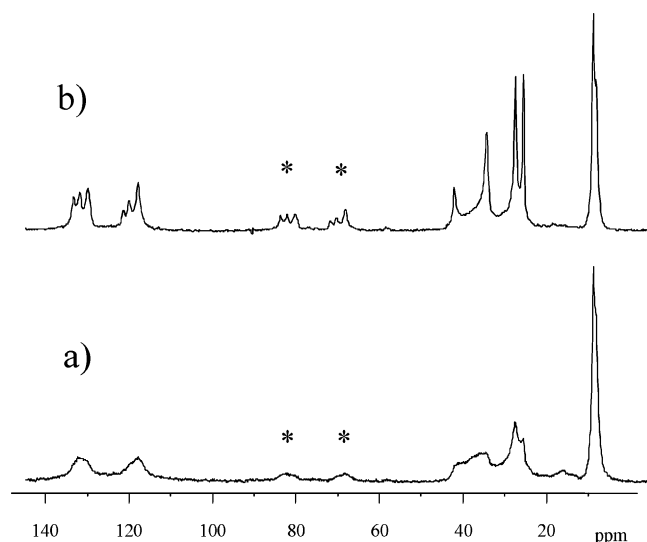
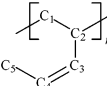


Figure 10. ^{13}C solid-state NMR spectra of (a) *cis*-1,2 syndiotactic polypentadiene, SPE spectrum, NS 4000; (b) *cis*-1,2 syndiotactic polypentadiene, CPMAS spectrum, NS 2000. Spinning sidebands indicated by (*).

Table 2. Assignment of the ^{13}C NMR Spectra of *cis*-1,2 Syndiotactic Polypentadiene in Solution and in the Solid State

Carbon	δ in ppm	
		
	solution	solid state
C1	42.54	47.37 39.48
C2	32.39	32.61 30.71
C3	137.06	138.58 136.97 135.07
C4	122.98	126.60 125.13 123.09
C5	13.33	13.90 13.32

three environments that are distinct both conformationally and with respect to packing. Because in all three environments C2 experiences two γ -gauche interactions, splittings are expected to be small as we indeed observe. However, for this structure, at least three signals are expected for C1, originating from 0, 1, and 2 γ -gauche interactions with the backbone. They occur respectively for the C1 atoms at the center of the two *tggt* and the *tttt* sequences (zero γ -gauche), in the two *tttg* sequences (one γ -gauche), and only one in the *gttg* sequence, experiencing two γ -gauche. The fact that only two signals are detected for the polymer under study, corresponding to 0 and 2 γ -gauche interactions, could be due to the presence of additional pseudo γ -gauche effects on the C1, which should have only one, determined by the side-chain conformation, thus modifying the expected three-signal pattern. Such additional gauche interactions indeed occur in the structure determined and refined from X-ray diffraction data for 1,2-syndiotactic poly(4-methyl-1,3-pentadiene),²³ in which a range of values was found for the side-chain torsion angles corresponding to C1–C2–C3–C4, some of them deviating by about 40° from the idealized skew confor-

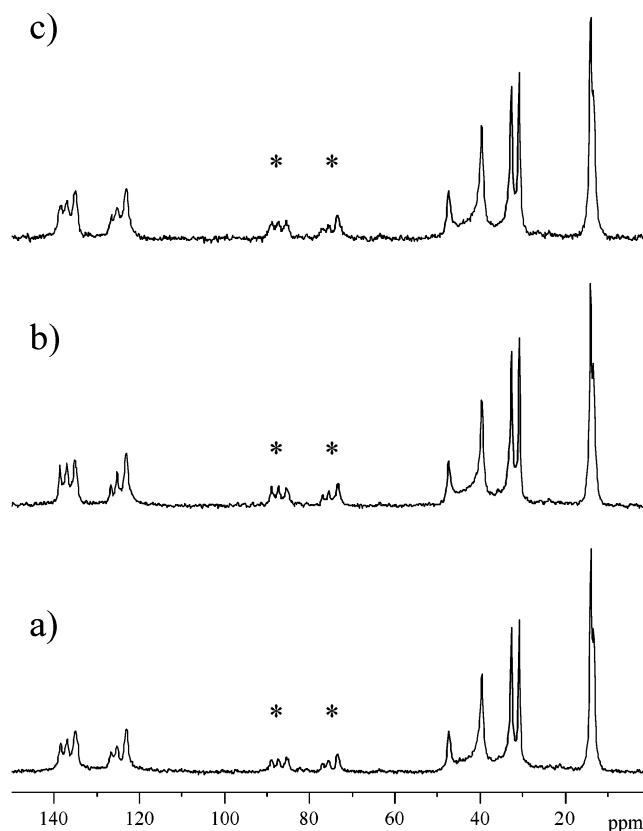


Figure 11. ^{13}C CPMAS NMR spectra of *cis*-1,2 syndiotactic polypentadiene fractions: (a) acetone soluble fraction, NS 840; (b) pentane soluble fraction, NS 128; and (c) residual fraction, NS 176. Spinning sidebands indicated by (*).

mation (adopted throughout Figures 12 and 13). The sharpness of the signals in the solid-state NMR spectra shown in Figures 10 and 11 makes this hypothesis, involving the exact coincidence of two of the three expected resonances, not very probable. The first conformation we have proposed, namely a nonuniform $(\text{T}_2\text{G}_2)_n$ helix thus remains more plausible, but the $\text{T}_6\text{G}_2\text{T}_2\text{G}_2$ conformation cannot be clearly ruled out with the available experimental data.

To help clarify the remaining ambiguity, molecular simulation investigations were carried out on *cis*-1,2 syndiotactic polypentadiene, 1,2-syndiotactic poly(4-methyl-1,3-pentadiene), and *trans*-1,2 syndiotactic polypentadiene, further specifying the general results already available in the literature.¹⁰ The stability of the three main expected minima were first evaluated with MM2 calculations on isolated chain fragments. The number of monomer units (up to 24) in the calculations ensured small terminal group effects on the resulting geometry, on the structures, and their relative stabilities. Starting from backbone conformations with standard torsion angles, i.e., 60° and 180°, the three main stationary points of the MM2 potential energy surface were confirmed. In the case of *cis*-1,2 syndiotactic polypentadiene, the structures correspond to T_4 (~164°), T_2G_2 (~–57° and ~170°), and $\text{T}_6\text{G}_2\text{T}_2\text{G}_2$ (47–61° and 170–176°) conformations. The internal energies were evaluated after appropriately taking into account termination contributions; the $\text{T}_6\text{G}_2\text{T}_2\text{G}_2$ and T_2G_2 conformations are very close in energy, i.e., the latter is favored by less than 0.1 kcal/(mol of CRU), and both are more stable by about 0.4 kcal/(mol of CRU) with respect to the T_4 structure. These results were com-

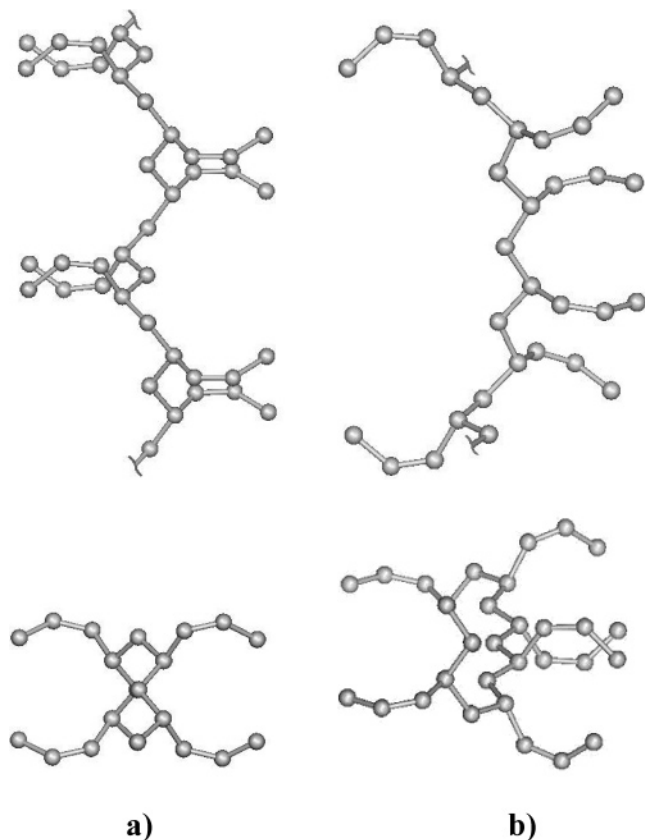


Figure 12. Side view and projection on a plane perpendicular to the chain axis of *cis*-1,2 syndiotactic polypentadiene in (a) the minimized T_2G_2 conformation constrained to a 7.5 Å periodicity and (b) the minimized $T_6G_2T_2G_2$ conformation with a 11.4 Å repeat. The two structures are nearly isoenergetic as the first structure is ca. 0.1 kcal/mol more stable than the second.

pleted by further molecular mechanics calculations, allowing building of infinite isolated chains with appropriate periodical conditions and symmetry constraints. In this second step, the PCFF force field as implemented in the Materials Studio package¹⁵ has been adopted. The PCFF minimization of the infinite T_2G_2 isolated chain was carried out, imposing a 7.5 Å axial periodicity and 2_1 symmetry (Figure 12a), while for the T_4 structure, the axial periodicity was 5.15 Å with glide symmetry (Figure 13a). The $T_6G_2T_2G_2$ structure was built with an axial periodicity axis of 11.40 Å imposing a C_2 axis through the methylene carbon at the center of the *ttttt* sequence (Figure 12b). The internal energy of the T_4 structure is higher by about 0.4 kcal/(mol of CRU) than that of the $(T_2G_2)_2$ helix, which is favored by less than 0.1 kcal/(mol of CRU) with respect to the $T_6G_2T_2G_2$ conformation in complete accordance with the unconstrained MM2 results on molecular fragments. The fact that no significant energy and geometrical differences resulted upon removing all the symmetry constraints, also in the case of the infinite chain models, supports the conclusion that the investigated structures represent stationary points. The different stability of the T_4 conformation is qualitatively apparent in significant torsion and bond angle distortions, which result in alleviating repulsive nonbonding interactions which would otherwise occur between side-chain methyl groups of adjacent CRUs (see Figure 13a).

To better evaluate the significance of the molecular modeling results, the described calculation scheme was applied to the 1,2-syndiotactic poly(4-methyl-1,3-pen-

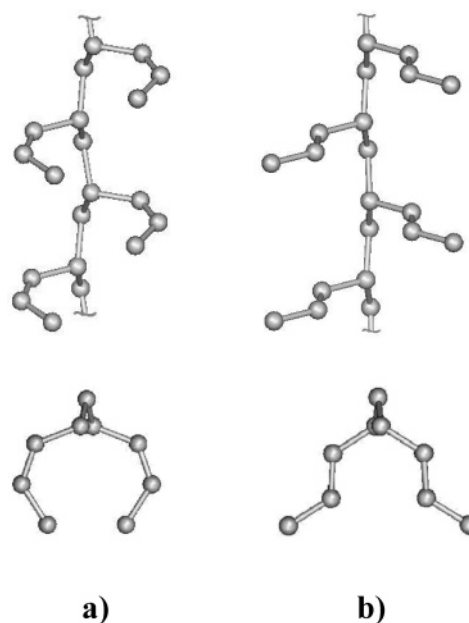


Figure 13. Side view and projection on a plane perpendicular to the chain axis of the minimized T_4 conformation constrained to a 5.15 Å periodicity of (a) *cis*-1,2 syndiotactic polypentadiene and (b) *trans*-1,2 syndiotactic polypentadiene. The first structure is distorted to alleviate steric conflict between the terminal methyls of the side chains of adjacent CRU and is ca. 0.5 kcal less stable than the two periodic conformations in Figure 12. The second represents the minimum energy periodic conformation for the *trans* polymer.

tadiene) system. As in the case of the *cis*-1,2 syndiotactic polypentadiene, using unconstrained MM2 molecular fragment minimization, the $T_6G_2T_2G_2$ and the T_2G_2 chain conformations show comparable stabilities, the second being more stable by about 0.2 kcal/(mol of CRU), while the T_4 structure has a higher internal energy (in this case, the energy gap is ca. 0.7 kcal/(mol of CRU)). With infinite chains constrained to appropriate symmetry and axial periodicity, the $T_6G_2T_2G_2$ and the T_2G_2 chain conformations, with 11.4 and 7.5 Å periodicities, become practically isoenergetic, whereas the T_4 conformation is destabilized by 0.5 kcal/(mol of CRU). The fact that the three conformers have closely similar energies closely corresponds to the experimental polymorphic behavior of this polymer as the observed stable polymorph adopts the $T_6G_2T_2G_2$ conformation, while in highly stretched fibers, minor amounts of a *trans* planar modification are apparent.²³ The reliability of the simulation scheme is additionally supported by the case of *trans*-syndiotactic 1,2-polypentadiene. The PCFF calculations, in accordance with MM2 results, demonstrate that, in this case, the stability order is reverted and the experimental T_4 structure with an axial periodicity of 5.15 Å (Figure 13b) is more stable by about 0.4 kcal/(mol of CRU) with respect to the T_2G_2 conformation (7.5 Å periodicity).

The discussed results appear unable to lead to unequivocal choices for the crystalline conformation of *cis*-1,2 syndiotactic polypentadiene. We should note here that, excluding the T_4 structure, the more extended $T_6G_2T_2G_2$ with a larger number of *transoid* conformational states is likely to be more stabilized over the T_2G_2 chain conformation by intermolecular packing contributions in the crystalline architecture. These effects may well determine a small bias favoring the $T_6G_2T_2G_2$ conformation with respect to the T_2G_2 conformation in the solid crystal structure, explaining the polymorphic

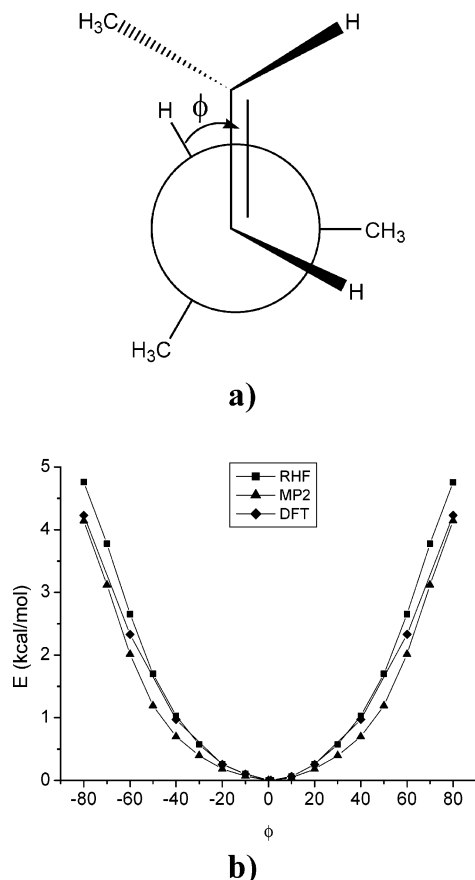


Figure 14. (a) Molecular fragment model adopted for the ab initio conformational analysis of the skew side-chain torsion angle $\phi = \text{C1-C2-C3-C4}$ of *cis*-1,2 syndiotactic polypentadiene. (b) RHF/6-31G**, MP2/6-31G**, and DFT/6-31G** potential energy plots as a function of the angle ϕ .

behavior of 1,2-syndiotactic poly(4-methyl-1,3-pentadiene). Because the $\text{T}_6\text{G}_2\text{T}_2\text{G}_2$ hypothesis involves, to be consistent with solid-state NMR results, substantial deviations of the side-chain conformation from the skew minimum, the energetic landscape around this minimum was investigated. RHF/6-31G**, MP2/6-31G**, and DFT/6-31G** ab initio calculations confirm that the skew conformation is the global minimum of the energy surface pertaining to the dihedral ϕ angle (see Figure 14a). The energy surface of the system (see Figure 14b) shows that even rotations of 40° around the global minimum correspond to energy penalties of about 0.5 kcal/mol, allowing the side chains some freedom in the crystalline architecture of the polymer.

Conclusions

The new polymer *cis*-1,2 syndiotactic polypentadiene has been obtained by polymerizing (*Z*)-1,3-pentadiene with the system $\text{CpTiCl}_3\text{-MAO}$ at low temperature. The polymer microstructure was attributed on the basis of a complete NMR and IR analysis. Because of the relatively low molecular weight of the polymer, it was impossible to determine structural and conformational features with standard diffraction approaches. Nevertheless, X-ray diffraction profiles suggest that a single crystalline phase is largely prevalent, and in this hypothesis, structural information could be obtained by solid-state ^{13}C NMR analysis. The data imply that the crystalline chain conformation of *cis*-1,2 syndiotactic polypentadiene involves at least two nonequivalent

methylene carbons, allowing us to exclude the all-trans T_4 conformation while suggesting a T_2G_2 type, possibly helical conformation, although the $\text{T}_6\text{G}_2\text{T}_2\text{G}_2$ cannot be excluded with full confidence. Indeed, the crystalline packing may influence the side-chain conformation, significantly perturbing expected solid-state ^{13}C NMR resonance multiplicities.

The experimental data and the results of conformational calculations confirm structural trends in 1,2-syndiotactic polydienes and polyolefins. Both the known systems with a *cis* carbon in the side-chain double bond, namely 1,2-syndiotactic poly(4-methyl-1,3-pentadiene) and *cis*-1,2 syndiotactic poly(1,3-pentadiene), show a conformational preference for the T_2G_2 and the $\text{T}_6\text{G}_2\text{T}_2\text{G}_2$ arrangements; indeed, the latter conformation was demonstrated in the crystals of the former polymer. In the present contribution, we supply substantial evidence that conformations of this kind occur in *cis*-1,2 poly(1,3-pentadiene) crystals. At variance, 1,2-syndiotactic polybutadiene²⁴ and 3,4-syndiotactic polyisoprene,²⁵ which carry sp^2 CH_2 -terminated side chains, adopt a T_4 main-chain conformation, similar to that found in polymers with a *trans* double bond in the side chains as the *trans* isomer of 1,2-syndiotactic polypentadiene.^{11b} The side-chain terminal *cis* methyl of 1,3-dienes polymerized to 1,2-syndiotactic polymers plays a crucial role, driving the main-chain away from all-*trans* conformational minima. The rationale of this behavior can be easily understood qualitatively with reference to Figure 13a. The steric conflict between the terminal *cis* methyls of the side chains of adjacent chemical repeats in the all-*trans* sequence are apparent; it can be alleviated because the *trans* segment is short in the $\text{T}_6\text{G}_2\text{T}_2\text{G}_2$ main-chain conformation (see Figure 12b). In an undistorted all-*trans* conformation, with the side chains arranged in the local conformational minima, these intermethyl distances would fall below 3 Å. To alleviate this steric conflict, cooperative distortions occur that account for the higher energy determined, even after minimization, for the all-*trans* as compared to the $\text{T}_6\text{G}_2\text{T}_2\text{G}_2$ and T_2G_2 conformation in both 1,2-poly(4-methyl-1,3-pentadiene) and *cis*-1,2-poly(1,3-pentadiene). In this perspective, these two polymers present analogies to syndiotactic polypropylene, syndiotactic polybutene, and other polymers with saturated side chains.²⁶

Acknowledgment. The authors acknowledge one of the anonymous reviewers for the insightful comments to the initially submitted manuscript, Dr. D. R. Ferro and Dr. M. Ragazzi for helpful discussion, and Dr. A. Boglia, Mr. Giulio Zannoni, and Mrs. F. Greco for their skillful assistance.

References and Notes

- (1) Natta, G.; Porri, L.; Mazzanti, G. (Montecatini SpA). Italian Patent 538453, 1956; *Chem. Abstr.* **1959**, *53*, 3756.
- (2) (a) Natta, G.; Porri, L.; Stoppa, G.; Allegra, G.; Ciampelli, F. *J. Polym. Sci., Part B* **1963**, *1*, 67. (b) Natta, G.; Porri, L.; Carbonaro, A.; Stoppa, G. *Makromol. Chem.* **1964**, *77*, 114. (c) Cabassi, F.; Italia, S.; Ricci, G.; Porri, L. In *Transition Metal Catalyzed Polymerization*; Quirk, R. P., Ed.; Harwood Academic: New York, 1988; pp 655–670. (d) Purevsuren, B.; Allegra, G.; Meille, S. V.; Farina, A.; Porri, L.; Ricci, G. *Polym. J.* **1998**, *30*, 431. (e) Porri, L.; Carbonaro, A. *Makromol. Chem.* **1963**, *60*, 236. (f) Natta, G.; Porri, L.; Carbonaro, A.; Ciampelli, F.; Allegra, G. *Makromol. Chem.* **1962**, *51*, 229. (g) Ricci, G.; Italia, S.; Comitani, C.; Porri, L. *Polym. Commun.* **1991**, *32*, 513.
- (3) Natta, G.; Porri, L.; Corradini, P.; Zanini, G.; Ciampelli, F. *J. Polym. Sci.* **1961**, *51*, 463.

- (4) Porri, L.; Di Corato, A.; Natta, G. *Eur. Polym. J.* **1969**, *5*, 1.
- (5) Beebe, D. H.; Gordon, C. E.; Thudium, R. N.; Throckmorton, M. C.; Hanlon, T. L. *J. Polym. Sci., Polym. Chem. Ed.* **1978**, *16*, 2285.
- (6) Sinn, H.; Kaminsky, W. *Adv. Organomet. Chem.* **1980**, *18*, 99.
- (7) Ricci, G.; Italia, S.; Giarrusso, A.; Porri, L. *J. Organomet. Chem.* **1993**, *451*, 67.
- (8) Ricci, G.; Italia, S.; Porri, L. *Macromolecules* **1994**, *27*, 868.
- (9) Porri, L.; Giarrusso, A.; Ricci, L. *Macromol. Symp.* **1995**, *89*, 383.
- (10) Pirozzi, B.; Napolitano, R.; Esposito, S. *Macromol. Theory Simul.* **2004**, *13*, 679.
- (11) (a) Ricci, G.; Forni, A.; Boglia, A.; Motta, T.; Zannoni, G.; Canetti, M.; Bertini, F. *Macromolecules* **2005**, *38*, 1064. (b) Ricci, G.; Motta, T.; Boglia, A.; Alberti, E.; Zetta, L.; Bertini, F.; Arosio, P.; Famulari, A.; Meille, S. V. *Macromolecules* **2005**, *38*, 8345.
- (12) Bax, A.; Freeman, R.; Frenkiel, T. A.; Levitt, M. H. *J. Magn. Reson.* **1981**, *43*, 478.
- (13) Aue, W. P.; Bartholdi, E.; Ernst, R. R. *J. Chem. Phys.* **1976**, *64*, 2229.
- (14) Allinger, N. L. *J. Comput. Chem.* **1993**, *14*, 755.
- (15) Materials Studio and Discover are products of Accelrys Inc. (see www.accelrys.com).
- (16) Frisch, M. J.; Trucks, G. W.; Schlegel, H. B.; Scuseria, G. E.; Robb, M. A.; Cheeseman, J. R.; Zakrzewski, V. G.; Montgomery, J. A., Jr.; Stratmann, R. E.; Burant, J. C.; Dapprich, S.; Millam, J. M.; Daniels, A. D.; Kudin, K. N.; Strain, M. C.; Farkas, O.; Tomasi, J.; Barone, V.; Cossi, M.; Cammi, R.; Mennucci, B.; Pomelli, C.; Adamo, C.; Clifford, S.; Ochterski, J.; Petersson, G. A.; Ayala, P. Y.; Cui, Q.; Morokuma, K.; Malick, D. K.; Rabuck, A. D.; Raghavachari, K.; Foresman, J. B.; Cioslowski, J.; Ortiz, J. V.; Stefanov, B. B.; Liu, G.; Liashenko, A.; Piskorz, P.; Komaromi, I.; Gomperts, R.; Martin, R. L.; Fox, D. J.; Keith, T.; Al-Laham, M. A.; Peng, C. Y.; Nanayakkara, A.; Gonzalez, C.; Challacombe, M.; Gill, P. M. W.; Johnson, B. G.; Chen, W.; Wong, M. W.; Andres, J. L.; Head-Gordon, M.; Replogle, E. S.; Pople, J. A. *Gaussian 98*, revision A.9; Gaussian, Inc.: Pittsburgh, PA, 1998.
- (17) (a) Zambelli, A.; Giongo, M. G.; Natta, G. *Makromol. Chem.* **1968**, *112*, 183. (b) See, for instance: Bovey, F. A. *High-Resolution NMR of Macromolecules*; Academic Press: New York, 1972.
- (18) Tonelli, A. E. In *NMR Spectroscopy and Polymer Microstructure: The Conformational Connection*; VCH: New York, 1989.
- (19) De Rosa, C.; Grassi, A.; Capitani, D. *Macromolecules* **1998**, *31*, 3163.
- (20) Belfiore, L. A.; Shilling, F. C.; Tonelli, A. E.; Lovinger, A. J.; Bovey, F. A. *Macromolecules* **1984**, *17*, 2561.
- (21) De Rosa, C.; Capitani, D.; Cosco, S. *Macromolecules* **1997**, *30*, 8322.
- (22) Chatani, Y.; Maruyama, H.; Asanuma, T.; Shiomura, T. *J. Polym. Sci., Polym. Phys. Ed.* **1991**, *29*, 1649.
- (23) (a) Ricci, G.; Italia, S.; Giarrusso, A.; Porri, L. *J. Organomet. Chem.* **1993**, *451*, 67. (b) Meille, S. V.; Capelli, S.; Ricci, G. *Macromol. Rapid Commun.* **1995**, *16*, 891. (c) Immirzi, A.; Tedesco, C.; Meille, S. V.; Famulari, A.; van Smaalen, S. *Macromolecules* **2003**, *36*, 3666.
- (24) Natta, G.; Corradini, P. *J. Polym. Sci.* **1956**, *20*, 251.
- (25) Bazzini, C.; Giarrusso, A.; Porri, L.; Pirozzi, B.; Napolitano, R. *Polymer* **2004**, *45*, 2871.
- (26) Corradini P.; De Rosa, C.; Pirozzi, B.; Venditto, V. *Gazz. Chim. Ital.* **1991**, *122*, 305.

MA047604Y